Journal of Technomaterial Physics
Journal homepage: https://talenta.usu.ac.id/JoTP

The Effect of Fe_3O_4 Addition on the Density and Porosity of Cellulose Nanofiber Aerogel Extracted by Oil Palm Trunk

Diana Alemin Barus* and Anindya Chandra Faizah
Department of Physics, Faculty of Mathematics and Natural Sciences, Universitas Sumatera Utara, Medan 20155, Indonesia.
*Corresponding Author: diana1@usu.ac.id

ARTICLE INFO

Article history:
Received 12 June 2023
Revised 18 August 2023
Accepted 25 August 2023
Available online 31 August 2023

E-ISSN: 2656-0755
P-ISSN: 2656-0747

How to cite:
D. A. Barus and A. C. Faizah, "The Effect of Fe_3O_4 Addition on the Density and Porosity of Cellulose Nanofiber Aerogel Extracted by Oil Palm Trunk," Journal of Technomaterial Physics, vol. 05, no. 02, pp. 50-55, Aug. 2023, doi: 10.32734/jotp.v5i2.12328.

ABSTRACT

This study investigates the influence of Fe_3O_4 addition on cellulose nanofiber aerogels' density and porosity characteristics. The cellulose nanofiber aerogels were synthesized with varying concentrations of Fe_3O_4: 0%, 0.25%, 0.5%, 0.75%, and 1%. The characterization of the cellulose nanofiber aerogels included physical tests to determine density and porosity and Fourier transform infrared (FTIR) analysis for functional group analysis. The results reveal a progressive increase in density from the lowest to the highest Fe_3O_4 concentrations: 0.115 g/cm^3, 0.135 g/cm^3, 0.162 g/cm^3, 0.163 g/cm^3, and 0.241 g/cm^3 for Fe_3O_4 concentrations of 0%, 0.25%, 0.5%, 0.75%, and 1%, respectively. Similarly, the porosity of the cellulose nanofiber aerogels exhibited a trend of decreasing values from the lowest to the highest Fe_3O_4 concentrations: 90.808%, 89.499%, 88.064%, 87.764%, and 82.844% for Fe_3O_4 concentrations of 0%, 0.25%, 0.5%, 0.75%, and 1%, respectively. Furthermore, FTIR analysis indicated that the structural integrity of the cellulose aerogels remained unchanged even after the incorporation of Fe_3O_4. While no new functional groups emerged, a discernible shift in wave numbers suggests the formation of bonds between the polymer network and Fe_3O_4. So, adding Fe_3O_4 to cellulose nanofiber aerogels led to notable alterations in density and porosity, while FTIR analysis confirmed the establishment of bonds between the polymer network and Fe_3O_4 without causing significant structural changes.

Keywords: Aerogel, Cellulose, Density, Fe_3O_4, Porosity

ABSTRAK

Penelitian ini menyelidiki pengaruh penambahan Fe_3O_4 terhadap karakteristik densitas dan porositas nanofiber selulosa. Aerogel nanofiber selulosa disintesis dengan variasi konsentrasi Fe_3O_4: 0%, 0,25%, 0,5%, 0,75%, dan 1%. Karakterisasi aerogel nanofiber selulosa meliputi uji fisik untuk menentukan densitas dan porositas dan analisis Fourier transform infrared (FTIR) untuk analisis gugus fungsi. Hasil menunjukkan peningkatan densitas secara progresif dari konsentrasi Fe_3O_4 terendah ke tertinggi: 0,115 g/cm^3, 0,135 g/cm^3, 0,162 g/cm^3, 0,163 g/cm^3, dan 0,241 g/cm^3 untuk konsentrasi Fe3O4 0%, 0,25 %, 0,5%, 0,75%, dan 1%, masing-masing. Demikian pula porositas aerogels nanofiber selulosa menunjukkan kecenderungan penurunan nilai dari konsentrasi Fe_3O_4 terendah hingga tertinggi: 90,808%, 89,499%, 88,064%, 87,764%, dan 82,844% untuk konsentrasi Fe_3O_4 0%, 0,25%, 0,5 %, 0,75%, dan 1%, masing-masing. Selanjutnya, analisis FTIR menunjukkan bahwa integritas struktural aerogel selulosa tetap tidak berubah bahkan setelah penggabungan Fe_3O_4. Meskipun tidak ada gugus fungsi baru yang muncul, pergeseran bilangan gelombang yang terlihat menunjukkan pembentukan ikatan antara jaringan polimer dan Fe_3O_4. Jadi, menambahkan Fe_3O_4 ke aerogels nanofiber selulosa menyebabkan perubahan penting dalam kepadatan dan porositas, sementara analisis FTIR mengonfirmasi pembentukan ikatan antara jaringan polimer dan Fe_3O_4 tanpa menyebabkan perubahan struktural yang signifikan.

Keywords: Aerogel, Selulosa, Densitas, Fe_3O_4, Porositas

http://doi.org/10.32734/jotp.v5i2.12328

1. Introduction

The oil palm tree (*Elaies guineensis*) is now one of Indonesia's most important agricultural plants and one of its main sources of income. More than 40 million tons of biomass are produced annually, and this lignocellulosic material offers a steady supply for the burgeoning oil palm biomass industry [1]. The palm oil processing industry produces a very large amount of solid waste. Several types of solid waste are produced, such as oil palm trunks (OPT), empty palm fruit bunches (EFB), palm kernel shells, and others. Waste from oil palms is a lignocellulosic substance that is high in cellulose. Every 25 to 30 years, during the replanting season, the trunks become available. The oil palm trunk's holo cellulose content ranges from 72 to 78%. This makes the trunks suitable to be used as raw material for cellulose aerogel production [2].

Cellulose is the most abundant polymer on earth, its structure is a linear polymer formed by D-glucose bonds and 1,4-β-glycosidic bonds. Cellulose and its derivatives have advantages such as thermal stability, chemical stability, easy to obtain, and cheap [3]. Cellulose nanofiber (CNF) is a derivative of cellulose which is described as a long, flexible fiber with high crystallinity, having a diameter of around 5-200 nm [4]. The advantages of CNF are the high tensile strength and intermolecular hydrogen bonds so that CNF is easily combined with other materials such as polymers [5]. There are various ways in the NSS isolation process, including using chemical methods such as alkaline treatment, enzymatic pretreatment, using ionic solutions, mediated oxidation using TEMPO (2,2,6,6-tetramethylpiperidine1-oxyl), and steam explosions. The NSS isolation process using chemical and enzymatic methods has the advantage of being proven effective and efficient with a crystallinity level of up to 60% [6].

Magnetic materials such as Fe_3O_4 are very attractive because of their highly specific surface, easy to recycle, and good thermal stability. This material has advantages due to its magnetic properties, catalytic electricity, and low toxicity. Aerogel is an adsorbent material that has good physical and chemical properties, such as low density (0,1-0,2i g/cm3) [7], high porosity (80-99.8%), and large specific surface area [8].

Aerogels have been synthesized from various materials such as inorganic aerogels [9], synthetic polymer-based aerogels [10], and natural polymer-based aerogels [11]. Polysaccharide-based aerogels formulated from natural ingredients are sustainable, biodegradable, and non-toxic [12]. In the synthesis method, freeze-drying was chosen because it is the simplest and most environmentally friendly method [13]. Therefore Fe_3O_4 has been widely used as a composite in adsorbent materials such as aerogels [14]. In this research, the synthesis of composite aerogel Fe_3O_4 reinforced by CNF will be carried out.

2. Method

2.1. Materials

Materials used in this study are oil palm trunks (OPT) obtained from Deli Serdang, Sumatera Utara, aquadest, sodium hydroxide (NaOH), hydrogen peroxide (H_2O_2), sulfuric acid (H_2SO_4), polyvinyl alcohol (PVA) and Fe_3O_4. All materials are used without further purification.

2.2. CNF Extraction

OPT that have been obtained are cut and blended into a powder. After that, the delignification process using an alkaline solution by adding 40 g of OPT powder into a 10% NaOH solution. It was then stirred at 300 rpm at 120℃ for 2 hours. Then, it was filtered and washed until it reached a neutral pH. Then, the bleaching process is carried out using a 10% H_2O_2 solution while stirring at 300 rpm at 120℃ for 2 hours, then filtered and washed until it reaches a neutral pH. The fiber obtained before was hydrolyzed using 30% H_2SO_4 solution while stirring at 300 rpm at 50℃ for 1 hour. The hydrolyzed fibers were washed using aquadest until they reached a neutral pH and then in the ultrasonic homogenizer for 1 hour.

2.3. Synthesis of CNF/Fe_3O_4 aerogel

Fe_3O_4 with each concentration of 0%; 0.25%; 0.5%, 0.75%, and 1% (w/v) was mixed into CNF suspension; then the suspension was ultrasonic homogenizer for 1 hour. After that, mix 5% PVA into the Fe_3O_4/NSS solution that has been ultrasonicated; after that, stir using a stir bar. Then the solution was printed using a silicon mold and put into the freezer at -12°C for 24 hours. The gel that has been formed is then put into the freeze dryer for 48 hours.

3. Results and Discussion

3.1. Density Test Result

The density of CNF/Fe_3O_4 aerogel can be determined with equation (1):

$$\rho = \frac{m}{V} \quad (1)$$

where m is the mass (g) obtained from weighing the CNF/Fe_3O_4 aerogel and V (cm^3) is obtained from the calculated aerogel dimension measurements using the cuboid equation. Aerogel densities are presented in Table 1.

Table 1. CNF/Fe_3O_4 aerogel densities under different Fe_3O_4 concentrations.

No	Fe_3O_4 Concentration	Mass (g)	Volume (cm^3)	Density (g/cm^3)
1	0%	0.0189	0.1642	0.115
2	0.25%	0.0262	0.1931	0.135
3	0.50%	0.0290	0.1782	0.162
4	0.75%	0.0245	0.1501	0.163
5	1%	0.0234	0.0971	0.241

It can be seen from Table 1 that the addition of Fe_3O_4 causes an increase in the density of CNF/Fe_3O_4 aerogel. The aerogel containing CNF/Fe_3O_4, ranging from the least to the most dense, was demonstrated using various concentrations of Fe_3O_4: 0%, 0.25%, 0.5%, 0.75%, and 1%. The corresponding densities for these concentrations were measured as 0.115 g/cm³, 0.135 g/cm³, 0.162 g/cm³, 0.163 g/cm³, and 0.241 g/cm³, respectively.

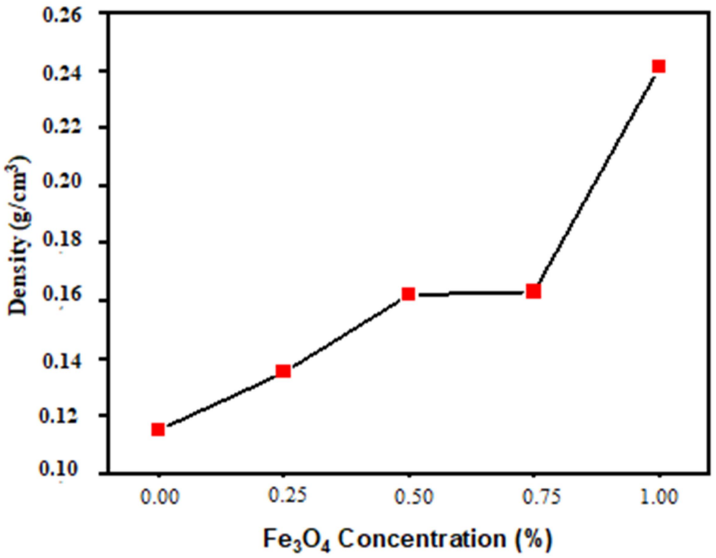

Figure 1. Graph of density values on variations in the addition of Fe_3O_4.

As depicted in Figure 1, the minimum density corresponds to the initial density achieved before introducing Fe3O4. The diminished density of the CNF aerogel underscores the light mass of the synthesized aerogel. The introduction of Fe_3O_4 concentration impacts the CNF aerogel's characteristics; higher concentrations lead to agglomeration, resulting in reduced pore size, as outlined in previous research [15].

3.2. Porosity Test Results

The porosity of CNF/Fe_3O_4 aerogels was calculated based on equation (2):

$$\varphi = \left(\frac{\rho_b - \rho_a}{\rho_b} \right) \times 100\% \quad (2)$$

where φ is the porosity of CNF/Fe_3O_4 aerogel (%), ρ_b is bulk density (g/cm^3) and ρ_a is the CNF/Fe_3O_4 aerogel density (g/cm^3).

For the value of the bulk density, the calculation used equation (3):

$$\rho_b = \frac{C_{NSS} + C_{PVA} + C_{Fe_3O_4}}{\frac{C_{NSS}}{\rho_{NSS}} + \frac{C_{PVA}}{\rho_{PVA}} + \frac{C_{Fe_3O_4}}{\rho_{Fe_3O_4}}} \quad (3)$$

Where C_{NNS} is the concentration of NNS (%), ρ_{NSS} is the cellulose nanofiber density (1.6 g/cm^3), C_{PVA} is the PVA concentration, ρ_{PVA} is the density of PVA (1.2 g/cm^3), $C_{Fe_3O_4}$ is the concentration of Fe_3O_4 (%) and $\rho_{Fe_3O_4}$ is the density of Fe_3O_4 (5.17 g/cm^3). From the (eq.2) obtained $\rho_{b\,0}$= 1.252 g/cm^3, $\rho_{b\,0.25}$ = 1.291 g/cm^3, $\rho_{b\,0.5}$ = 1.329 g/cm^3, $\rho_{b\,0.75}$= 1.367 g/cm^3, $\rho_{b\,1}$= 1.404 g/cm^3. Based on the calculation, CNF/Fe_3O_4 aerogel porosities are presented in Table 2.

Table 2. CNF/Fe_3O_4 aerogel densities under different Fe_3O_4 concentrations.

No	Fe_3O_4 Concentration	Porosity (%)
1	0%	90.808
2	0.25%	89.499
3	0.50%	87.764
4	0.75%	88.064
5	1%	82.844

The data in Table 2 reveals a descending order of porosity, with the highest to lowest values observed in the 1%, 0.5%, 0.75%, 0.25%, and 0% samples, corresponding to 82.844%, 87.764%, 88.064%, 89.4999%, and 90.808% respectively. Porosity and density exhibit an inverse relationship: heightened porosity decreases density. This phenomenon arises from the abundance of pores in high-porosity materials, contributing to the reduced weight of the cellulose aerogel [16].

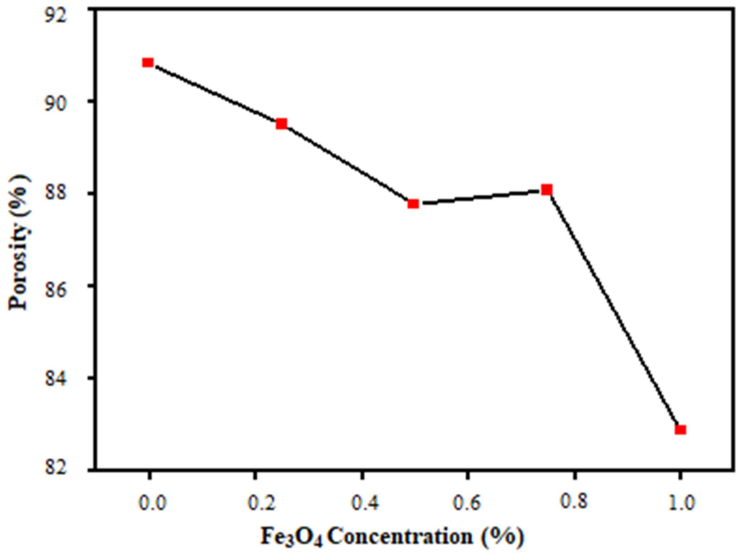

Figure 2. Graph of porosity values on variations in the addition of Fe_3O_4.

As depicted in Figure 2, the CNF/Fe_3O_4 aerogel with the most minor porosity is achieved by altering Fe_3O_4 concentration at 1%, indicating a reduced number of pores compared to the aerogel prior to Fe_3O_4 addition. The porosity levels of the aerogel are affected by the introduction of Fe_3O_4. The overall density within each composition influences the porosity value blend. The concentration of Fe_3O_4 solution corresponds to a decrease in the quantity of water employed in the solution [16]. In this investigation, the porosity of the cellulose aerogels demonstrates an upward trend as the Fe_3O_4 concentration diminishes in each specimen. This phenomenon is attributed to the impact of the cross-linker agent employed within the solution [17].

3.3. Fourier Transform Infra-Red analysis

Figure 3 shows the FTIR spectra of the CNF/Fe_3O_4 aerogel; for the Fe_3O_4 sample, the absorption peak was observed at wave number 3,265 cm^{-1}, which indicated the presence of –OH groups where the observed hydroxyl groups were found in cellulose isolated from oil palm trunk [18]. Furthermore, absorption peaks at

wavenumber 2,320 cm^{-1} and 2,109 cm^{-1} indicated C-H bending originating from the acetate group in the PVA matrix [19]. Next, at the absorption peaks of 1,635 cm^{-1} and 1,274 cm^{-1}, it was observed that the strain vibrations of C=O came from the -COO group present in the vinyl acetate monomer in PVA and the strain vibrations of C-O contained in the PVA matrix [20]. In the 0.5% AKFE sample, there was a shift from the -OH absorption peak, which shifted from wave number 3,254 cm^{-1} to 3,265 cm^{-1}, which was associated with stretching of the hydroxy groups in the NSS or the intermolecular bonds between PVA and NSS. Furthermore, there was a shift in the absorption peak of wave number 1,640 cm^{-1}, indicating that a bond had formed between PVA and NSS bonds between PVA and CNF. Furthermore, there was a shift in the absorption peak of wave number 1,840 cm^{-1}, indicating that a bond had formed between PVA and NSS [21].

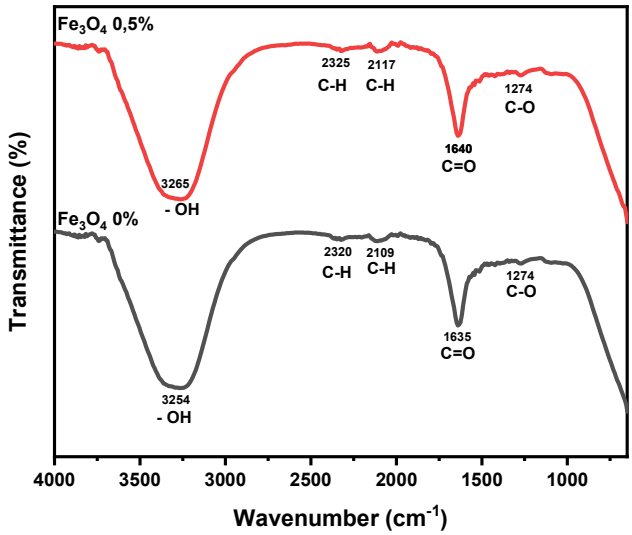

Figure 3. FTIR spectrum curves of the CNF/ Fe_3O_4 aerogel.

Testing is also carried out by charging the smartphone battery using the manufacturer's charger, the smartphone is connected to PLN's electric current so that a comparison of time spent in charging the smartphone battery can be seen.

4. Conclusion

Based on the preceding results, it can be deduced that CNF/Fe_3O_4 aerogel exhibits low density within the range of 0.1-0.2 g/cm³ and high porosity ranging from 82% to 90%. The introduction of Fe_3O_4 has a discernible impact on aerogel density and porosity, leading to an increase in density and a decrease in porosity. The minimum density is observed in aerogels with 0% Fe_3O_4 variation, while the maximum density is found in those with 1% Fe_3O_4 variation. Conversely, the greatest porosity is achieved in aerogels with 0% Fe_3O_4 variation, while the lowest porosity is associated with 1% Fe_3O_4 variation. Furthermore, Fourier-Transform Infrared (FT-IR) analysis conducted on cellulose aerogels after the addition of Fe_3O_4 reveals a shift in wavenumber, indicating the formation of bonds between the polymer network and Fe_3O_4

References

[1] Badan Pusat Statistik, “Produksi Tanaman Perkebunan (Ribu Ton), 2019-2021,” *Badan Pusat Statistik*, 2021.

[2] J. Lamaming, R. Hashim, O. Sulaiman, C. P. Leh, T. Sugimoto, and N. A. Nordin, "Cellulose nanocrystals isolated from oil palm trunk," *Carbohydr Polym*, vol. 127, pp. 202–208, Aug. 2015, doi: 10.1016/j.carbpol.2015.03.043.

[3] K. Kumar, S. Srivastav, and V. S. Sharanagat, "Ultrasound assisted extraction (UAE) of bioactive compounds from fruit and vegetable processing by-products: A review," *Ultrason Sonochem*, vol. 70, p. 105325, Jan. 2021, doi: 10.1016/j.ultsonch.2020.105325.

[4] G. Lazorenko, A. Kasprzhitskii, V. Mischinenko, and A. Kruglikov, "Fabrication and characterization of metakaolin-based geopolymer composites reinforced with cellulose nanofibrils," *Mater Lett*, vol. 308, p. 131146, Feb. 2022, doi: 10.1016/j.matlet.2021.131146.

[5] R. Kango, Hadiyanto, and H. Pongtularan. 2021. Design and implementation of a solar integration in electric smart, *AIP Conference Proceedings,* vol. 1088, no. 012058.
[6] A. R. Nafisah *et al.*, "Synthesis of Cellulose Nanofiber from Palm Oil Empty Fruit Bunches Using Acid Hydrolysis Method," 2022. [Online]. Available: http://journal.unnes.ac.id/sju/index.php/ijcs
[7] S. Iswar *et al.*, "Dense and strong, but superinsulating silica aerogel," *Acta Mater*, vol. 213, p. 116959, Jul. 2021, doi: 10.1016/j.actamat.2021.116959.
[8] L. Y. Long, Y. X. Weng, and Y. Z. Wang, "Cellulose aerogels: Synthesis, applications, and prospects," *Polymers*, vol. 8, no. 6. MDPI AG, Jun. 06, 2018. doi: 10.3390/polym10060623.
[9] F. Jiang, S. Hu, and Y. Hsieh, "Aqueous Synthesis of Compressible and Thermally Stable Cellulose Nanofibril–Silica Aerogel for CO_2 Adsorption," *ACS Appl Nano Mater*, vol. 1, no. 12, pp. 6701–6710, Dec. 2018, doi: 10.1021/acsanm.8b01515..
[10] B. N. Nguyen, M. A. B. Meador, D. Scheiman, and L. McCorkle, "Polyimide Aerogels Using Triisocyanate as Cross-linker," *ACS Appl Mater Interfaces*, vol. 9, no. 32, pp. 27313–27321, Aug. 2017, doi: 10.1021/acsami.7b07821.
[11] F. Zhu, "Starch based aerogels: Production, properties and applications," *Trends Food Sci Technol*, vol. 89, pp. 1–10, Jul. 2019, doi: 10.1016/j.tifs.2019.05.001.
[12] Z. Liu, S. Zhang, B. He, S. Wang, and F. Kong, "Synthesis of cellulose aerogels as promising carriers for drug delivery: a review," *Cellulose*, vol. 28, no. 5. Springer Science and Business Media B.V., pp. 2697–2714, Mar. 01, 2021. doi: 10.1007/s10570-021-03734-9.
[13] M. E. El-Naggar, S. I. Othman, A. A. Allam, and O. M. Morsy, "Synthesis, drying process and medical application of polysaccharide-based aerogels," *International Journal of Biological Macromolecules*, vol. 145. Elsevier B.V., pp. 1115–1128, Feb. 15, 2020. doi: 10.1016/j.ijbiomac.2019.10.037.
[14] B. S. Damasceno, A. F. V. da Silva, and A. C. V. de Araújo, "Dye adsorption onto magnetic and superparamagnetic Fe3O4 nanoparticles: A detailed comparative study," *J Environ Chem Eng*, vol. 8, no. 5, p. 103994, Oct. 2020, doi: 10.1016/j.jece.2020.103994.
[15] B. A. A. Prakasa and Sam Matahari, "SINTESA SUPERABSORBEN AEROGEL SELULOSA DARI KERTAS BEKAS," Institut Teknologi Sepuluh Nopember, Surabaya, 2015.
[16] Diana Eka Pratiwi, Sulfikar, and Gusma Harfiana Abbas, "Sintesis dan Karakterisasi Aerogel Selulosa dari Limbah Ampas Sagu," *SEMINAR NASIONAL HASIL PENELITIAN 2022*, pp. 684–698, 2022.
[17] B. Y. Gustinenda and Kautsar Cakrawala Margo, "SINTESIS SUPERABSORBEN AEROGEL SELULOSA BERBASIS SABUT KELAPA," Institut Teknologi Sepuluh Nopember, Surabaya, 2017.
[18] J. Lamaming, R. Hashim, C. P. Leh, O. Sulaiman, and T. Sugimoto, "Chemical, Crystallinity and Morphological Properties of Oil Palm Trunk Parenchyma and Vascular Bundle," *International Journal of Environmental Engineering-IJEE*, vol. 2, no. 1, 2015.
[19] Y. Okahisa, K. Matsuoka, K. Yamada, and I. Wataoka, "Comparison of polyvinyl alcohol films reinforced with cellulose nanofibers derived from oil palm by impregnating and casting methods," *Carbohydr Polym*, vol. 250, p. 116907, Dec. 2020, doi: 10.1016/j.carbpol.2020.116907.
[20] M. M. Abudabbus *et al.*, "Biological activity of electrochemically synthesized silver doped polyvinyl alcohol/graphene composite hydrogel discs for biomedical applications," *Compos B Eng*, vol. 104, pp. 26–34, Nov. 2016, doi: 10.1016/j.compositesb.2016.08.024.
[21] T. Zhou, X. Cheng, Y. Pan, C. Li, and L. Gong, "Mechanical performance and thermal stability of polyvinyl alcohol–cellulose aerogels by freeze drying," *Cellulose*, vol. 26, no. 3, pp. 1747–1755, Feb. 2019.